

# A Numerical Study on the Influence of CO<sub>2</sub> Dilution on Combustion Characteristics of a Turbulent Diffusion Flame

Yasaman Tohidi, Rouzbeh Riazi, Shidvash Vakilipour, Masoud Mohammadi

**Abstract**—The objective of the present study is to numerically investigate the effect of CO<sub>2</sub> replacement of N<sub>2</sub> in air stream on the flame characteristics of the CH<sub>4</sub> turbulent diffusion flame. The Open source Field Operation and Manipulation (OpenFOAM) has been used as the computational tool. In this regard, laminar flamelet and modified k- $\epsilon$  models have been utilized as combustion and turbulence models, respectively. Results reveal that the presence of CO<sub>2</sub> in air stream changes the flame shape and maximum flame temperature. Also, CO<sub>2</sub> dilution causes an increment in CO mass fraction.

**Keywords**—CH<sub>4</sub> diffusion flame, CO<sub>2</sub> dilution, OpenFOAM, turbulent flame.

## I. INTRODUCTION

THE global warming issue has become a major concern in recent years. Increasing the level of carbon dioxide, as a prominent contributor to global warming, and other pollutant emissions in the atmosphere leads to significant climate changes and can be detrimental for human health [1]. In this regard, using different strategies to reduce emission levels seems unavoidable. In practical applications, the addition of CO<sub>2</sub> as a diluent to fuel or oxidizer stream is commonly used to decrease flame temperature and achieve lower pollutant emissions [2], [3]. As CO<sub>2</sub> is a combustion product, it can be easily extracted from exhaust gas by condensing water vapor exists in the combustion products. CO<sub>2</sub> dilution has a significant impact on the flame structure, flammability limits, and pollutant emissions. Several researchers have investigated the effect of CO<sub>2</sub> dilution on flame characteristics.

Liu et al. [4] depicted that CO<sub>2</sub> addition affects the flame structure and soot formation through dilution, thermal and chemical effects. Park et al. [5] studied the effect of different diluents in methane-air counterflow diffusion flames and showed that thermal effect of CO<sub>2</sub> addition leads to the flame temperature reduction. Etere et al. [6] considered the effect of CO<sub>2</sub> dilution on the structure and pollutant emissions of methane-air turbulent diffusion flames. They found that, with the higher diluent concentrations in the fuel stream, visible flame length, flame temperature, and consequently soot and NO<sub>x</sub> emissions are reduced, but it leads to an increase in CO

concentration. Zhuo et al. [7] conducted a numerical study on the impact of N<sub>2</sub>, CO<sub>2</sub>, and H<sub>2</sub>O addition on combustion characteristics of syngas turbulent non-premixed jet flames. Their results indicated that CO<sub>2</sub> diluted flames have the largest reduction of flame temperature among other diluents. Also, they showed that the CO<sub>2</sub> addition shortens the flame size. Lock et al. [8] compared the impact of fuel stream with air stream dilution by CO<sub>2</sub> on the lift-off process of methane-air coflow flames. Wang et al. [9] performed a numerical investigation on the physical and chemical effects of CO<sub>2</sub> and H<sub>2</sub>O additives in the methane diffusion flames. They focused on the thermal and chemical effects of these diluents on the flame temperature and Emission Index of CO (EICO). Xu et al. [10] investigated the effect of H<sub>2</sub>O and CO<sub>2</sub> diluted oxidizer on the structure and shape of coflow diffusion flames. They reported that the thermal and chemical effects of CO<sub>2</sub> replacement of N<sub>2</sub> in air would lead to the reduction of flame temperature. Gascoin et al. [11] considered the effect of CO<sub>2</sub> dilution on the flame temperature distribution. Furthermore, several researchers studied the effect of CO<sub>2</sub> dilution on flammability limits and some emissions such as NO<sub>x</sub> [12]-[14].

The objective of current computational research is mainly to investigate the effect of CO<sub>2</sub> addition to oxidizer stream on the flame length, temperature distribution, and CO concentration in a certain bluff-body stabilized methane swirling flame [21].

## II. THE OPENFOAM FRAMEWORK

Open source Field Operation and Manipulation (OpenFOAM) is an open source CFD software package written in C++. It contains numerous solvers which are designed to solve complex fluid flows involving combustion, turbulence, and heat transfer. It also includes tools for meshing and utilities for post-processing and data manipulation. This package has been developed by OpenCFD Ltd. at ESI Group and distributed by the OpenFOAM Foundation [16].

## III. COMBUSTION MODEL

In this research, the steady laminar flamelet model (SLFM) implemented in OpenFOAM has been used as combustion model [22]. SLFM is based on the assumption that the turbulent flames can be considered as an ensemble of small laminar diffusion flames named as flamelets, in which the chemical reaction zone is thin enough compared to the turbulent length scales [17]. One of the most important

Yasaman Tohidi, Rouzbeh Riazi, and Masoud Mohammadi are with the Department of Aerospace Engineering, Faculty of New Sciences and Technologies, University of Tehran, Tehran, Iran (e-mail: yas.tohidi@ut.ac.ir, ro\_riazi@ut.ac.ir, mas.mohammadi@ut.ac.ir).

Shidvash Vakilipour is with the Department of Aerospace Engineering, Faculty of New Sciences and Technologies, University of Tehran, Tehran, Iran (phone: 989121326951, e-mail: vakilipour@ut.ac.ir).

advantages of the flamelet model is that the flamelets calculation is independent of turbulent flow in the pre-processing step. In pre-processing step, flamelets are stored in a flamelet library. After that, thermodynamic properties and species mass fractions can be extracted from these tables using parameters such as mixture fraction ( $Z$ ), its variance ( $Z''$ ) and scalar dissipation rate ( $\chi$ ), transported in the turbulent code. The conservation equations of species mass fraction and temperature in the mixture fraction space can be written as:

$$\rho \frac{\partial y_k}{\partial t} - \frac{1}{2} \rho \chi \frac{\partial^2 y_k}{\partial Z^2} - \omega_k = 0 \quad (1)$$

$$\rho \frac{\partial T}{\partial t} - \frac{1}{2} \rho \chi \left( \frac{\partial^2 T}{\partial Z^2} + \frac{1}{c_p} \frac{\partial c_p}{\partial Z} \frac{\partial T}{\partial Z} \right) + \frac{1}{c_p} \sum_{k=1}^n h_k \omega_k = 0 \quad (2)$$

where  $\rho$  is the thermodynamic density,  $Y_k$  is the chemical species mass fraction,  $T$  denotes the temperature,  $c_p$  and  $h_k$  are the specific isobaric heat capacity and the specific enthalpy of species  $k$ , respectively. The chemical species source term which is marked by  $\omega_k$  can be calculated with the chemistry reaction mechanism. The scalar dissipation rate,  $\chi$ , is regarded as an inverse diffusion time scale.

$$\chi = 2D \left( \frac{\partial Z}{\partial y} \right)^2 \quad (3)$$

$\chi$  is the function of mixture fraction and can be parameterized by its value at stoichiometric mixture,  $\chi_{st}$ . In the current study, the flamelets are computed via the open-source chemistry software Cantera in which the scalar dissipation rate is adjusted by changing mass flow at fuel and oxidizer inlets.

Then, the mean value for species mass fraction and temperature are calculated by using Favre Presumed Probability Density Function (PDF).

$$\bar{Y}_k = \int_0^1 \int_0^1 Y_k(Z, \chi_{st}) P(Z, \chi_{st}) \partial Z \partial \chi_{st} \quad (4)$$

$$\bar{T}_k = \int_0^1 \int_0^1 T(Z, \chi_{st}) P(Z, \chi_{st}) \partial Z \partial \chi_{st} \quad (5)$$

Two additional transport equations for the mean mixture fraction and its variance have to be solved.

$$\frac{\partial \bar{\rho} \bar{Z}}{\partial t} + \frac{\partial \bar{\rho} \bar{u}_i \bar{Z}}{\partial x_i} = \frac{\partial}{\partial x_i} \left( \mu_{eff} \frac{\partial \bar{Z}}{\partial x_i} \right) \quad (6)$$

$$\frac{\partial \bar{\rho} \overline{\partial Z'^2}}{\partial t} + \frac{\partial \bar{\rho} \bar{u}_i \overline{\partial Z'^2}}{\partial x_i} = \frac{\partial}{\partial x_i} \left( \mu_{eff} \frac{\partial \overline{\partial Z'^2}}{\partial x_i} \right) + 2\mu_{eff} \left( \frac{\partial \bar{Z}}{\partial x_i} \right)^2 - \bar{\rho} \bar{\chi} \quad (7)$$

Here, the effective viscosity is consisted of a laminar and a turbulent contribution ( $\mu_{eff} = \mu + \mu_t$ ) in which the eddy viscosity ( $\mu_t$ ) can be calculated by using a turbulence model.

The mean scalar dissipation rate in the mixture fraction variance equation can be modeled as:

$$\bar{\chi} = C_\chi \frac{\varepsilon}{k} \bar{Z}'' \quad (8)$$

$C_\chi = 2$ . Also here,  $k$  and  $\varepsilon$  are the turbulent kinetic energy

and its dissipation respectively. In this study, the chemical reaction mechanism applied for the  $\text{CH}_4$  combustion is GRI 2.11 with 49 species and 277 reactions [18].

#### IV. MODIFIED K-EPSILON TURBULENCE MODEL

Among the several turbulence models which have been employed for simulation of the bluff-body swirl flames, the modified k-epsilon model (by changing the constant  $C_{\epsilon 1}$  from 1.44 to 1.6) has been proposed to improve the prediction of flow field and compensate for excessive diffusion [19], [20].

#### V. NUMERICAL MODELING

The experimental data obtained by Al-Abdeli and Masri [21] was used for validation purpose. The schematic of burner is depicted in Fig. 1. The swirl burner is located in wind tunnel with about 2% free stream turbulence and the area of 130 mm square.

The 60 mm-diameter swirling annulus which provides the flow of pure air encompasses the stream of a fuel jet and a ceramic bluff-body face. In the other words, fuel and oxidizer are separated by a bluff-body which generates recirculation zones in the flow field [23]. The diameter of the fuel jet and the bluff-body face is 3.6 and  $D=50$  mm, respectively.

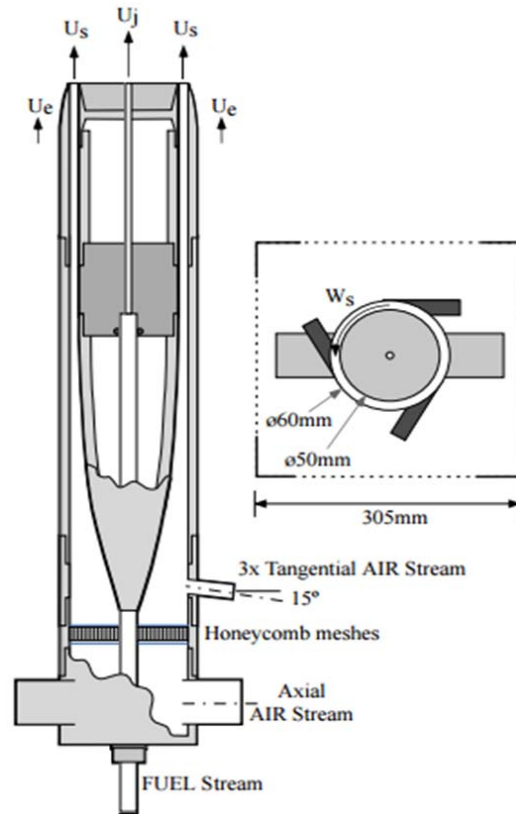


Fig. 1 The schematic of burner [24]

The boundary condition and flow properties of the reacting field such as the fuel jet velocity ( $U_j$ ), the axial annular velocity ( $U_s$ ), the tangential annular velocity ( $W_s$ ), and the

velocity of co-flow air stream in the wind tunnel ( $U_c$ ) are listed in Table I.

In the current research, the swirl number is set to be  $W_s/U_s=0.5$ . Also, the Reynolds numbers of fuel jet and swirl air flow are considered to be 7200 and 75900, respectively.

TABLE I  
FLOW PROPERTIES

| case        | Fuel    | oxidizer | $U_j$<br>(m/s) | $U_s$<br>(m/s) | $W_s$<br>(m/s) | $U_c$<br>(m/s) |
|-------------|---------|----------|----------------|----------------|----------------|----------------|
| Swirl flame | Methane | air      | 32.7           | 38.2           | 19.1           | 20             |

A 2-D wedge-type computational domain which is discretized into 45000 cells (180 and 250 cells in radial and axial directions respectively) has been considered in this simulation. To obtain a better accuracy, a mesh structure with higher resolution close to the wall and inlet boundaries are

defined.

Fig. 2 shows the configuration of 2-D wedge-type grid. The flow field should be fully-developed at the exit plane. For this reason, the inlet flow streams are extended upstream of the exit plane to  $D=50$  mm. In the current research, the OpenFOAM has been used as the computational toolbox. The code solves Favre-averaged Navier-Stokes and continuity equations. The Reynolds stresses are closed using modified  $k$ -epsilon model. The PISO algorithm is utilized for pressure-velocity coupling.

A Dirichlet condition is applied in the inlet for the velocity and mixture fraction fields, and a Neumann condition is set in the outlet boundary. Also, the pressure is fixed in the outlet and side boundaries, while a Neumann condition is applied for the inflow.

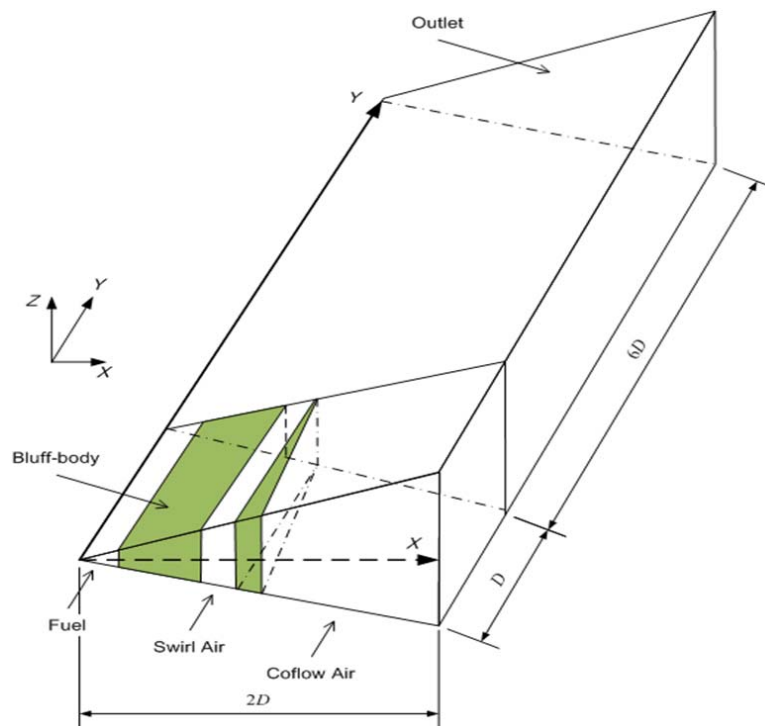


Fig. 2 The configuration of 2-D wedge-type computational domain

## VI. RESULTS AND DISCUSSION

### A. Grid Dependency

The grid independency study has been done by changing the number of cells from 15000 to 75000 considering a mesh structure with higher resolution in the regions with high gradient of swirl velocity. This is because the most deviation from experimental data has been observed in the regions with higher velocity gradients. In Fig. 3, the effects of three different grids on the velocity and temperature profiles have been investigated in certain axial locations.

Although the grid with 15000 cells is unable to predict the aforementioned profiles properly, the difference between the simulation results of 45000 and 75000 cells is negligible, and

no significant changes are observed in the simulation results. Consequently, the grid with 45000 cells has been utilized in this study.

### B. Validation

Simulation results are compared with experimental data and previous studies [15] for temperature, axial and circumferential velocity components, and these results are depicted in Figs. 4-6. This comparison reveals that the predicted results are in a good agreement with the measurements and the general trend of profiles can be captured with an acceptable accuracy. It is worth mentioning that a similar level of accuracy has already been reported regarding the simulation of this swirl flame in previous related

studies [15]. Fig. 4 compares the calculated axial velocity component with measurements in different axial locations. It shows some inaccurate predictions around the centerline. This can be explained considering the low capability of RANS models regarding the simulation of shear flows.

### C. Effect of CO<sub>2</sub> Addition to the Air Stream

The main objective of this research is the study of CO<sub>2</sub> addition to the air stream and its effect on the flame length, flame temperature distribution and CO mass fraction. To achieve this aim, different amounts of CO<sub>2</sub> are added to the air. The velocity boundary condition and the jet nozzle diameter kept unchanged and consequently, the mass flow rate of the air stream increases by CO<sub>2</sub> addition.

There are different definitions for the non-premixed turbulent flame length (L). The first one is that it can be determined based on the visible flame length. The second definition is that the flame length would be the axial location of peak temperature on the centerline. Also, the third definition states that flame length is considered as axial distance in which the mixture fraction would be stoichiometric on the centerline.

Since the studied flame structure in the present research has

an hourglass shape, the farthest stoichiometric mixture fraction point is not always on the centerline. In this regard, the flame length is defined as the largest vertical distance between the nozzle exit plane and the stoichiometric mixture fraction point [15].

The details of different CO<sub>2</sub> dilution cases are depicted in Table II. The flame length is decreased slightly with the addition of CO<sub>2</sub>. Actually, by CO<sub>2</sub> replacement of N<sub>2</sub> (i.e. by addition of CO<sub>2</sub>), the density of oxidizer is increased and this could lead to increment of the oxidizer momentum. The slight increase in the momentum of oxidizer flow may result in production of stronger recirculation zones in the flow field which can increase the degree of mixing. This increment in mixing may lead to the reduction of flame length.

TABLE II  
THE PERCENTAGE OF DILUTION AND CORRESPONDING DATA IN DIFFERENT CASES

| Case   | oxidizer Composition                                     | Z <sub>st</sub> | L/D   |
|--------|--|-----------------|-------|
| Case 1 | 10%CO <sub>2</sub> +69%N <sub>2</sub> +21%O <sub>2</sub> | 0.0528          | 2.060 |
| Case 2 | 15%CO <sub>2</sub> +64%N <sub>2</sub> +21%O <sub>2</sub> | 0.0512          | 2.032 |
| Case 3 | 20%CO <sub>2</sub> +59%N <sub>2</sub> +21%O <sub>2</sub> | 0.0498          | 2.016 |

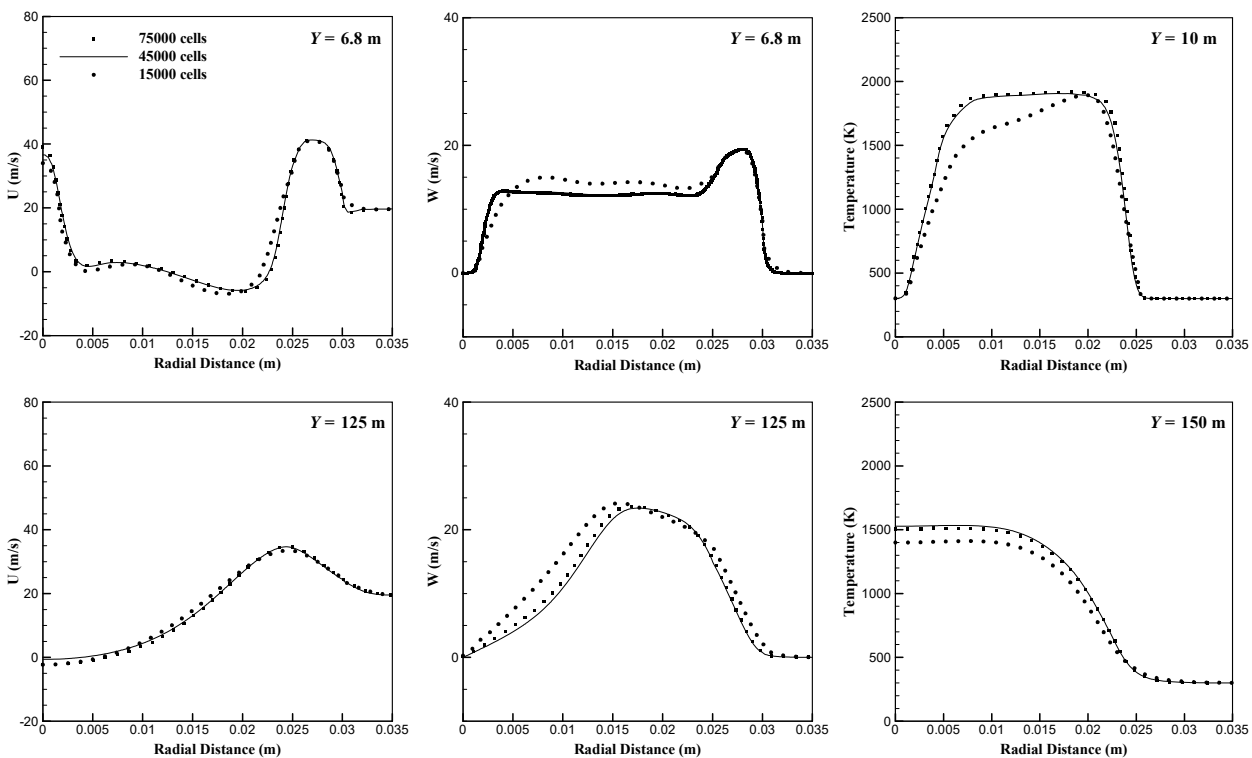


Fig. 3 Grid resolution study for radial profile of predicted temperature and velocity components at different axial locations using three mesh structure with 15000, 45000, and 75000 cells

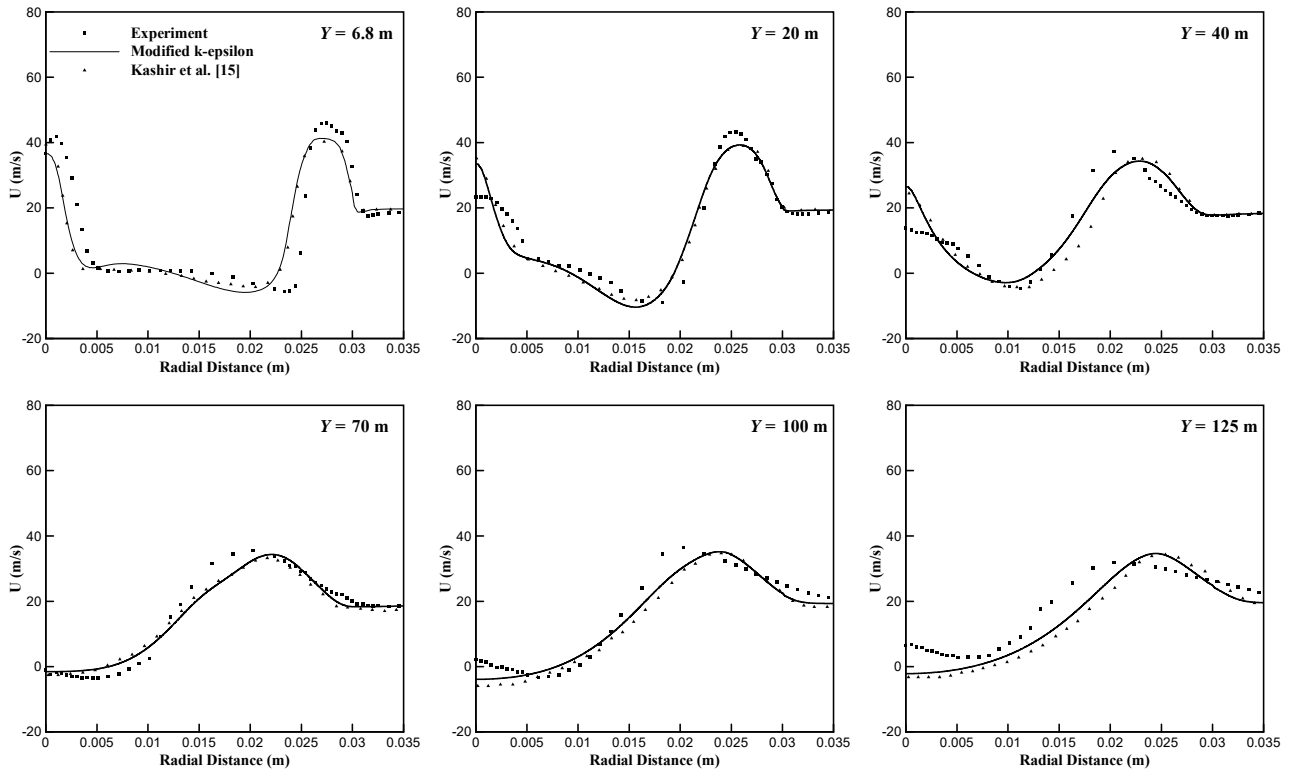


Fig. 4 Radial profile of predicted axial velocity component compared with measurements at different axial locations

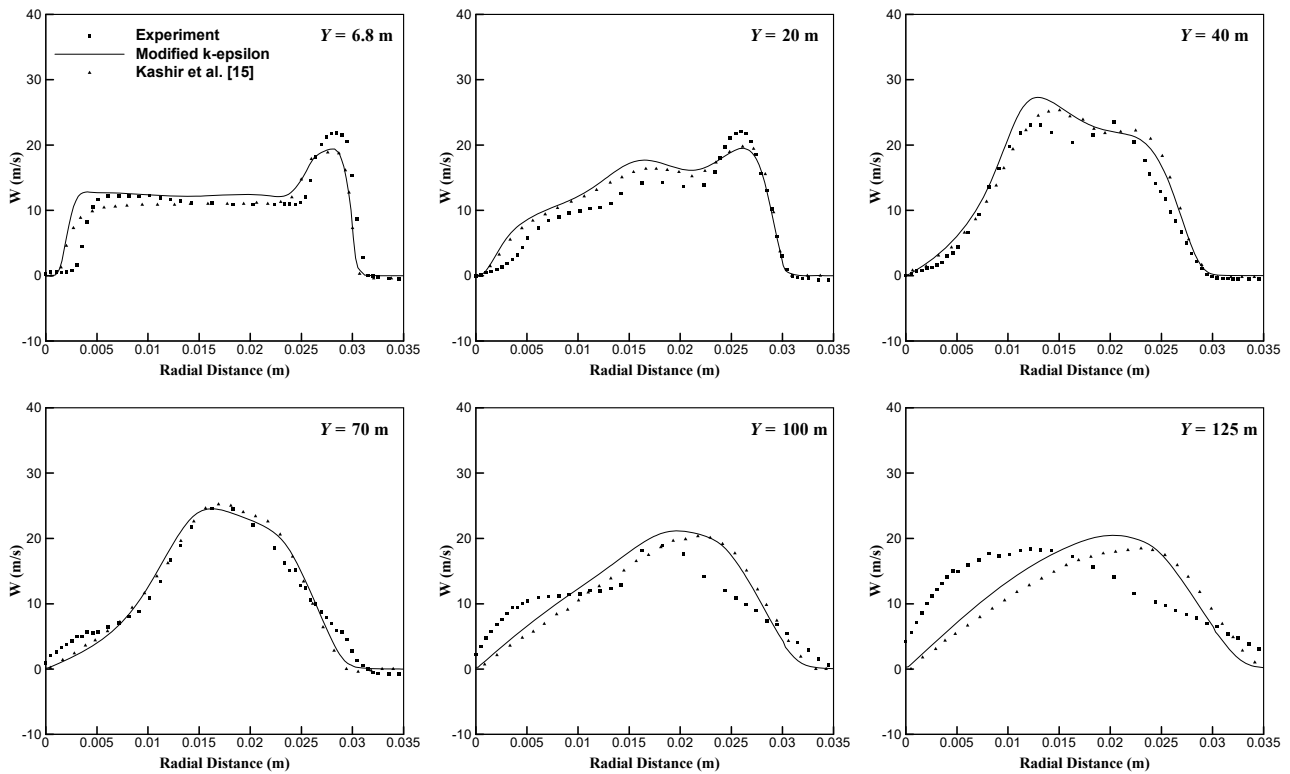


Fig. 5 Radial profile of predicted circumferential velocity component compared with measurements at different axial locations

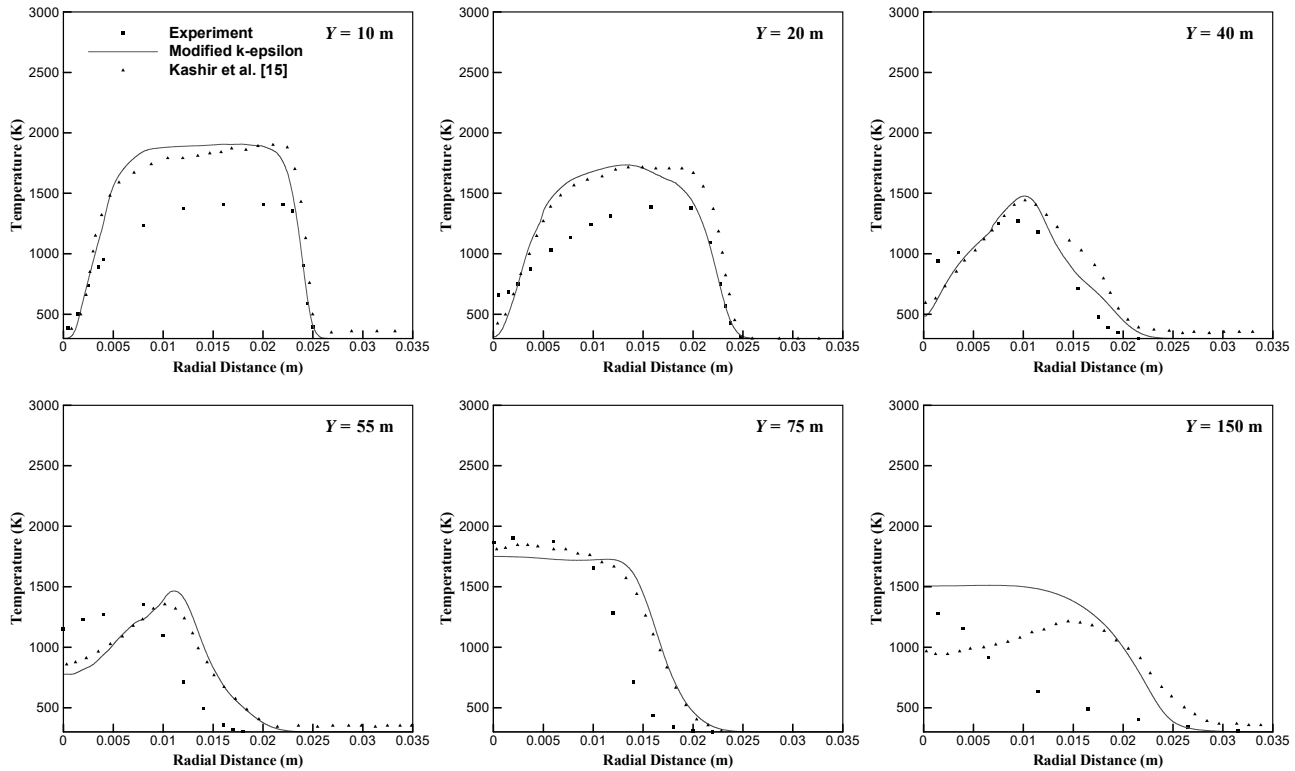


Fig. 6 Radial profile of predicted temperature compared with measurements at different axial locations

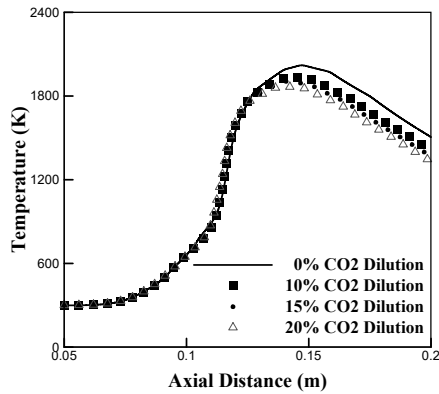


Fig. 7 Effect of  $\text{CO}_2$  dilution on the flame temperature distribution along the centerline of nozzle

The effect of  $\text{CO}_2$  addition instead of  $\text{N}_2$  on the flame temperature distribution along the centerline is depicted in Fig. 7. This figure indicates that the temperature decreases by addition of  $\text{CO}_2$ . It is worth mentioning that, compared with the case of no  $\text{CO}_2$  dilution, the peak temperature in Fig. 7 reduces around 83, 117, and 151 K by adding the amount of 10%, 15% and 20% of  $\text{CO}_2$ , respectively.

This can be explained by the higher heat capacity of  $\text{CO}_2$  compared with  $\text{N}_2$  which can lead to the reduction of flame temperature [10], [11], [14]. It is also interesting that the maximum flame temperature on the centerline (which can be assumed as a measure of flame length) moves toward the

upstream of flow.

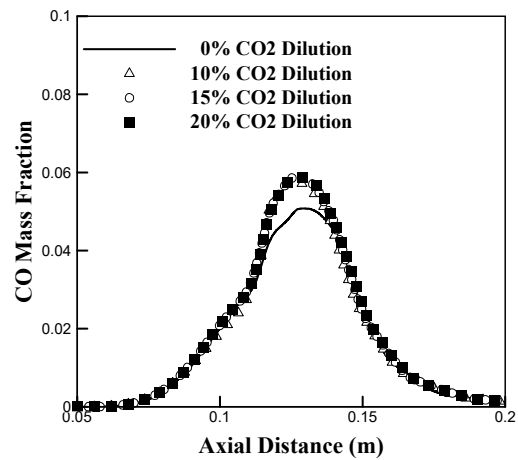


Fig. 8 Effect of  $\text{CO}_2$  dilution on the CO Mass Fraction distribution along the centerline of nozzle

Fig. 8 shows the radial profile of CO mass fraction distribution on the centerline of flow field. This figure demonstrates that increase of  $\text{CO}_2$  (compared with the case of no  $\text{CO}_2$  dilution) leads to the increment of CO mass fraction in a certain region along the centerline. It is also interesting that, based on the calculations, a recirculation zone is created in the same region. This increase of CO mass fraction with addition of  $\text{CO}_2$  might be due to the reduction of temperature in this

region (please see Fig 7).

## VII. CONCLUSION

The effect of CO<sub>2</sub> replacement of N<sub>2</sub> on the characteristics of a turbulent diffusion flame was studied numerically. The OpenFOAM platform has been utilized as the computational tool. At the first stage, the simulation results were compared with reported experimental data and previous related studies. The comparisons revealed that predicted results were in good agreement with the measurements and simulations were able to capture the general trend of temperature and velocity component profiles with an acceptable accuracy. After the validation process, the effect of CO<sub>2</sub> addition to air stream was investigated. Results showed that the flame length and the maximum flame temperature were reduced by addition of CO<sub>2</sub>. Furthermore, CO<sub>2</sub> dilution led to the increase of CO mass fraction.

## REFERENCES

- [1] Pope III CA, Ezzati M, Dockery DW. Fine-particulate air pollution and life expectancy in the United States. *N Engl J Med*. 2009 Jan 22;209(360):376-86.
- [2] Liu CY, Chen G, Sipöcz N, Assadi M, Bai XS. Characteristics of oxy-fuel combustion in gas turbines. *Applied Energy*. 2012 Jan 31;89(1):387-94.
- [3] Zheng M, Reader GT, Hawley JG. Diesel engine exhaust gas recirculation—a review on advanced and novel concepts. *Energy conversion and management*. 2004 Apr 30;45(6):883-900.
- [4] Liu F, Guo H, Smallwood GJ, Gülder ÖL. The chemical effects of carbon dioxide as an additive in an ethylene diffusion flame: implications for soot and NO<sub>x</sub> formation. *Combustion and Flame*. 2001 Apr 30;125(1):778-87.
- [5] Park J, Kim SG, Lee KM, Kim TK. Chemical effect of diluents on flame structure and NO emission characteristic in methane-air counterflow diffusion flame. *International Journal of Energy Research*. 2002 Oct 25;26(13):1141-60.
- [6] Erete JI, Hughes KJ, Ma L, Fairweather M, Pourkashanian M, Williams A. Effect of CO<sub>2</sub> dilution on the structure and emissions from turbulent, non-premixed methane-air jet flames. *Journal of the Energy Institute*. 2017 Apr 30;90(2):191-200.
- [7] Zhuo L, Jiang Y, Qiu R, An J, Xu W. Effects of Fuel-Side N<sub>2</sub>, CO<sub>2</sub>, H<sub>2</sub>O Dilution on Combustion Characteristics and NO<sub>x</sub> Formation of Syngas Turbulent Nonpremixed Jet Flames. *Journal of Engineering for Gas Turbines and Power*. 2014 Jun 1;136(6):061505.
- [8] Lock A, Briones AM, Aggarwal SK, Puri IK, Hegde U. Liftoff and extinction characteristics of fuel-and air-stream-diluted methane-air flames. *Combustion and flame*. 2007 Jun 30;149(4):340-52.
- [9] Wang L, Liu Z, Chen S, Zheng C, Li J. Physical and chemical effects of CO<sub>2</sub> and H<sub>2</sub>O additives on counterflow diffusion flame burning methane. *Energy & fuels*. 2013 Dec 9;27(12):7602-11.
- [10] Xu H, Liu F, Sun S, Zhao Y, Meng S, Tang W. Effects of H<sub>2</sub>O and CO<sub>2</sub> diluted oxidizer on the structure and shape of laminar coflow syngas diffusion flames. *Combustion and Flame*. 2017 Mar 31;177:67-78.
- [11] Gascoin N, Yang Q, Chetehouna K. Thermal effects of CO<sub>2</sub> on the NO<sub>x</sub> formation behavior in the CH<sub>4</sub> diffusion combustion system. *Applied Thermal Engineering*. 2017 Jan 5;110:144-9.
- [12] Gu M, Chu H, Liu F. Effects of simultaneous hydrogen enrichment and carbon dioxide dilution of fuel on soot formation in an axisymmetric coflow laminar ethylene/air diffusion flame. *Combustion and Flame*. 2016 Apr 30;166:216-28.
- [13] Yu B, Lee S, Lee CE. Study of NO<sub>x</sub> emission characteristics in CH<sub>4</sub>/air non-premixed flames with exhaust gas recirculation. *Energy*. 2015 Nov 30;91:119-27.
- [14] Roy RN, Sreedhara S. A numerical study on the influence of airstream dilution and jet velocity on NO emission characteristics of CH<sub>4</sub> and DME bluff-body flames. *Fuel*. 2015 Feb 15;142:73-80.
- [15] Kashir B, Tabejamaat S, Jalalati N. A numerical study on combustion characteristics of blended methane-hydrogen bluff-body stabilized swirl diffusion flames. *International Journal of Hydrogen Energy*. 2015 May 18;40(18):6243-58.
- [16] URL <http://www.openfoam.org>. (No date).
- [17] Peters N. *Turbulent Combustion*. Cambridge University Press; 2000.
- [18] URL [http://www.me.berkeley.edu/gri\\_mech/](http://www.me.berkeley.edu/gri_mech/). (Accessed 3 November 1995).
- [19] Dally BB, Fletcher DF, Masri AR. Flow and mixing fields of turbulent bluff-body jets and flames. *Combustion Theory and Modelling*. 1998 Jun 1;2(2):193-219.
- [20] Sreedhara S, Huh KY. Modeling of turbulent, two-dimensional nonpremixed CH<sub>4</sub>/H<sub>2</sub> flame over a bluffbody using first-and second-order elliptic conditional moment closures. *Combustion and flame*. 2005 Oct 31;143(1):119-34.
- [21] Al-Abdeli YM, Masri AR. Stability characteristics and flowfields of turbulent non-premixed swirling flames. *Combustion Theory and Modelling*. 2003 Dec 1;7(4):731-66.
- [22] Müller HA, Ferraro F, Pfitzner M. Implementation of a Steady Laminar Flamelet Model for non-premixed combustion in LES and RANS simulations. In 8th International OpenFOAM Workshop 2013 Jun 11.
- [23] Poinot T, Veynante D. *Theoretical and numerical combustion*. RT Edwards, Inc.; 2005.
- [24] Kalt PA, Al-Abdeli YM, Masri AR, Barlow RS. Swirling turbulent non-premixed flames of methane: flow field and compositional structure. *Proceedings of the Combustion Institute*. 2002 Jan 1;29(2):1913-9.